JOURNAL OF APPLIED ENGINEERING SCIENCES
ISSN: 2247-3769 / e-ISSN: 2284-7197

VOL. 15(28), ISSUE 2/2025
ART.NO. 464 pp. 285-292

A STUDY ON THE DESIGN OF NOZZLES WITH A HIGH AIR ENTRAINMENT RATIO

F. Ozkan[a], Begum Kantarci Onay[a], A. Baylar[b, *]

[a] Department of Civil Engineering, Firat University, Elazig, Turkey, E-mails: fozkan@firat.edu.tr, begumkantarci@hotmail.com
[b*] Department of Civil Engineering, Eskisehir Technical University, Eskisehir, Turkey, E-mail: abaylar@eskisehir.edu.tr

Received: 28.04.2025 / Accepted: 28.06.2025 / Revised: 30.10.2025 / Available online: 15.12.2025

DOI: 10.2478/jaes-2025-0034

KEY WORDS: air entrainment, nozzle, two-phase flow, water jet.

ABSTRACT:

When a water jet passes through a layer of air and plunges into a pool of water, it is well known that it entrains a significant amount of air into the pool. This forms a submerged, two-phase region with a large surface area at the air-water interface. This process is called plunging water jet entrainment and aeration. This paper describes an experimental study of the air entrainment ratio of two-hole circular nozzles. Depending on which air holes were opened on the circular nozzles, negative pressure was created. The resulting aeration of the jet affected its expansion, shape, and roughness; consequently, it also affected the air entrainment ratio. The investigation showed that the maximum air entrainment ratio was achieved with a nozzle length four times the diameter of the nozzle. Higher air entrainment ratios were observed for air holes with diameters greater than 2 mm. Additionally, a design equation was developed to estimate the air entrainment ratio of two-hole circular nozzles. This equation considers the ratio of the nozzle diameter to the air hole diameter, the water jet length, the circular nozzle length, and the jet velocity at the nozzle inlet.

1. INTRODUCTION

A liquid can be aerated by entrainment, which occurs when another liquid with the same or different properties impinges on its surface. Examples include a jet plunging into a pool, a breaking wave plunging into the ocean, and a droplet impinging on a liquid surface. This aeration system, which is based on air entrainment by a plunging liquid jet, has several advantages over conventional aeration systems: it does not require an air compressor, it is simple to construct and operate, it is free from operational difficulties such as clogging in air diffusers, and it does not require mechanical aerators. The phenomenon of air being entrapped in a plunging liquid jet has been observed in various engineering disciplines, including hydraulic, nuclear, marine hydrodynamics, and wastewater treatment engineering. Recently, there has been growing interest in aeration by water jets plunging into pools. This process is energetically attractive as a means of direct contact in contaminated or hazardous environments.

When a water jet impinges on a receiving pool at rest, air bubbles can be entrained and carried way below the free surface of the pool. This process is called entrainment and aeration. A water jet impinging on a pool of water causes air entrainment when the jet velocity exceeds a critical value. The jet impact process can create intense turbulence and entrain a large amount of air into the plunging pool. The entrained air quickly bursts into small bubbles that interact with the surrounding liquid flow. This creates a complex, turbulent, two-phase mixing flow that enhances mass and heat transfer between the gas and liquid phases.

A considerable number of researchers have studied the air entrainment rate (Q_a) of plunging water jets. Experimental studies of the air entrainment rate of plunging water jets were conducted by van De Sande and Smith (1973 and 1976), McKeogh and Ervine (1981), and Sene (1988). Kusabiraki et al. (1990a and 1990b) studied the effect of nozzles with different values of length-to-diameter ratio on the air entrainment rate. These and the other related studies were reviewed by Bin (1993). Evans et al. (1996) measured the change in effective jet diameter as a function of free jet length for vertical water jets passing through air. Recently, Oguz (1998), Zhu et al. (2000) and Ohl et al. (2000) investigated the role of surface disturbances in the entrainment of bubbles by water jets. Yamagiwa et al. (2000) studied the effect of nozzle contracted angle on the air entrainment rate of a vertical plunging water jet.

Baylar and Emiroglu (2004) conducted an experimental study of the air entrainment rate and oxygen transfer efficiency of circular nozzles with and without air holes. Specifically, the study examined the effect of varying the number, positions, and open/closed status of the air holes. The results of the study indicated that circular nozzles with air holes had superior air entrainment rates and oxygen transfer efficiencies compared to those without air holes. Among all the nozzles studied, those with two air holes had the highest air entrainment rates. In addition, Bagatur and Baylar (1998), Bagatur et al. (2002), Emiroglu and Baylar (2003a, 2003b), Baylar and Emiroglu (2003), Baylar et al. (2005, 2006, 2007a, 2007b, 2008, 2009, 2010a, 2010b), and Ozkan et al. (2006) conducted numerous studies on the air

* Corresponding author: Ahmet Baylar, Department of Civil Engineering, Eskisehir Technical University, 26555 Eskisehir, Turkey, E-mail: abaylar@eskisehir.edu.tr

entrainment rate and oxygen transfer efficiency of the nozzle type.

Qu et al. (2013) conducted an experimental study to characterize a liquid impinging jet on a pool and the resulting entrainment process using various non-invasive flow visualization techniques and image analysis. The 2D velocity distribution and instantaneous flow dynamic behaviour of a submerged and an impinging jet for the non-entrainment regime below the interface were obtained using particle image velocimetry (PIV). Fu et al. (2022) performed numerical simulations and experimental tests for the jet flow field of square nozzles with different length-to-diameter ratios and contraction angles. The results showed that a smaller length-to-diameter ratio and a smaller contraction angle of the nozzle resulted in better jet cohesion and lower dynamic pressure in the constant-velocity core area, which was more suitable for long-distance, low-pressure water jet operations.

Miwa et al. (2018) investigated the air entrainment rate of a vertically plunging liquid jet. Three types of liquids with different physical properties were used as working fluids for the experiment. A total of 1690 data points were obtained to investigate the entrainment behaviour. From the experimental observation, the alcohol-water mixture tended to produce much finer bubbles compared to the water and sucrose-water mixtures. Miwa et al. (2019) investigated the air entrainment rate of an inclined liquid jet plunging into a pool. Three types of liquids with different physical properties in terms of viscosity and surface tension were used. A total of 3110 data points were obtained using water at room temperature, an alcohol-water mixture, and a sucrose-water mixture. From the database, a new semi-empirical model for the air entrainment ratio for inclined liquid jets was developed.

Ma et al. (2020) conducted an experimental study on air entrainment by inclined circular plunging water jets from long nozzles with different jet impingement heights up to 6.1 m. The results showed that for plunging water jets with the same hydraulic head, the air entrainment rate first increased with increasing jet impingement height and then decreased with further increasing jet impingement height. The early increase in air entrainment rate was caused by the increase in jet surface roughness, while the later decrease was caused by the disintegration of the water jet. The impinging jet momentum decreased dramatically due to the reduced mass and the significant energy dissipation through the atmosphere caused by jet disintegration. This resulted in a much smaller penetration depth and air entrainment rate compared to a continuous jet.

Salehi et al. (2022) presented detailed computational fluid dynamics simulations of air entrainment phenomena occurring during the filling process of a hydraulic brake column. The computational fluid dynamics model was first validated against measured data for a water jet plunging into a pool of water. For this purpose, both volume-of-fluid and Eulerian multifluid models were tested. It was found that both models accurately predicted the geometric parameters of the cavity at the pinch point. Satisfactory agreement was also obtained between the computational fluid dynamics data and the measurements for both the penetration length and the penetration velocity. Tang et al. (2022) conducted a two-dimensional numerical simulation to investigate the air-water flow properties and turbulence characteristics of vertically supported planar plunging jets. Three jet impact velocities were investigated for the same jet length. The simulated distributions of time-averaged vertical velocities and void fraction at different depths below the impingement point were presented and compared with the existing experimental data, showing overall satisfactory agreement.

Alazmi et al. (2023) experimentally investigated the effects of key parameters on the air entrainment rate in a confined plunging liquid jet reactor. Different downcomer diameters, jet lengths, liquid flow rates, nozzle diameters, and jet velocities were used to measure the air entrainment rate. The non-linear relationship between the air entrainment rate and the confined plunging jet reactor parameters suggested that the application of unconventional regression algorithms to predict the air entrainment rate was appropriate. In addition to the experimental work, machine learning algorithms were applied to the confined plunging jet reactor parameters to determine the parameter that best predicts the air entrainment rate.

Kandukuri et al. (2024) investigated the characteristics of the cavity produced and the amount of air entrained by the initial impact of a plunging water jet on a stationary water surface. The characteristics of the cavity were analysed through experimental studies, and it was found that existing correlations developed for the impact of the bulge introduced into a continuous jet do not accurately capture the characteristics of the initial impact cavity. Therefore, new semi-analytical correlations explicitly adapted to the initial impact characteristics were developed. The correlation coefficients were estimated from the experimental data. Furthermore, numerical simulations of the plunging jet flow with three different jet lengths were performed to verify the applicability of these correlations at other velocities. The results showed good agreement between the numerical and experimental data and the newly developed correlations.

This paper describes an experimental study of the air entrainment ratio of two-hole circular nozzles. The effect of the ratio of nozzle diameter to air hole diameter, water jet length, circular nozzle length, and jet velocity at the nozzle inlet on the air entrainment ratio was investigated.

2. MECHANISM OF AIR ENTRAINMENT AT IMPINGING WATER JETS

McKeogh and Ervine (1981) described four basic air entrainment mechanisms with respect to circular jets. They classified the air entrainment mechanisms as: 1- Annular oscillation; 2- Intermittent vortex; 3- Turbulent occlusion; and 4- Droplet entrainment. A description of these stages is shown in Figure 1a-d.

1- Laminar jets (see Figure 1a) are relatively smooth and form an oscillating annulus at the plunging point. The annulus typically extends several jet diameters below the pool surface. Air entrainment occurs when the annulus breaks apart from the jet.

2- When the jet characteristics are in transition between laminar and turbulent (see Figure 1b), the intermittent vortex mechanisms occur. In this case, an indentation of the pool surface appears around the jet periphery. The indentation is caused by a combination of the downward flow of the jet and the pressure of the air in the boundary layer surrounding the jet. The intermittent vortex indentation does not extend as far below the surface as the oscillating annulus and is not as sharply curved. A free vortex causes inward radial flow (see Figure 1b, inset). It is difficult to define the exact range of Reynolds numbers within which this type of air entrainment occurs because the laminar properties of the jet depend not only on the Reynolds number but also on the shape of the nozzle.

3- When a fully turbulent jet impinges on the pool, the indentation on the surface becomes highly irregular in form due to the rough jet periphery. The intense roughness of the liquid surface and the impact point trap ambient air. The air captured by the above processes is distributed by diffusion in the form of bubbles as shown in Figure 1c.

4- As the water jet falls freely, it reaches a point where the solid mass of falling water is completely disintegrated. The jet then falls in the form of discrete water droplets that entrain air upon impact with the pool. The streamlines around the growing cavity resemble the lines of force around one end of a magnet, as shown in Figure 1d.

Koga (1982) pointed out that the intermittent vortex mechanism described by McKeogh and Ervine (1981) is similar in angled water jets. However, there are some differences between vertical jets operating in the intermittent regime and the acute jets studied by Koga (1982). Jets impinging at 90° and operating in the intermittent vortex regime have a cylindrically symmetric indentation similar to the indentation observed by Koga (1982). However, the indentation is not cylindrically symmetric at acute angles. In angled water jets, a flow is observed that returns surface bubbles to the plunging point. At acute angles, the cylindrical symmetry is no longer present, but there is a similar surface flow. Figure 2 (inset) illustrates the surface bubble path for acute jets. The dashed lines outline the region where the bubbles surface. The arrows indicate the path taken by surface bubbles approaching the plunging point.

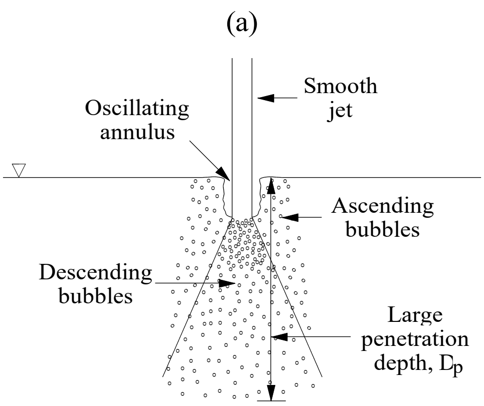

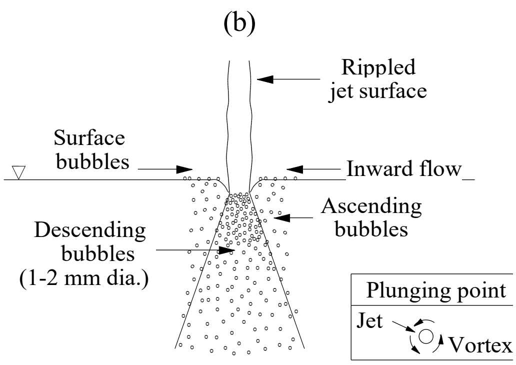

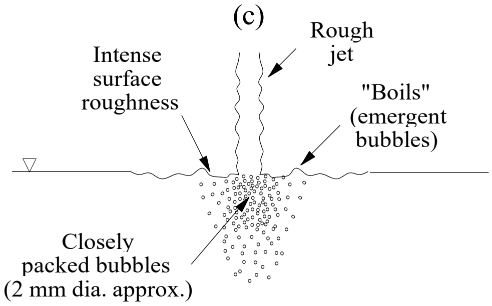

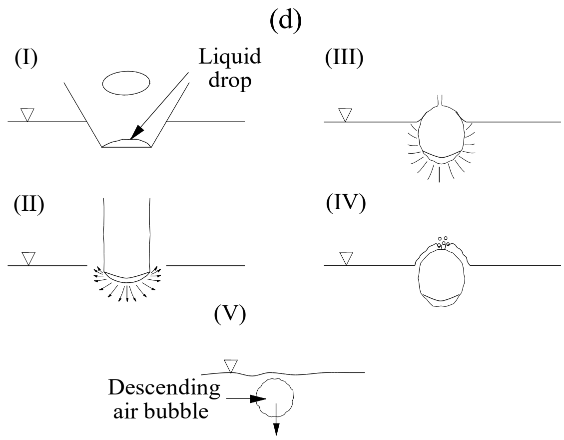

Figure 1. Mechanism of air entrainment at impinging water jets

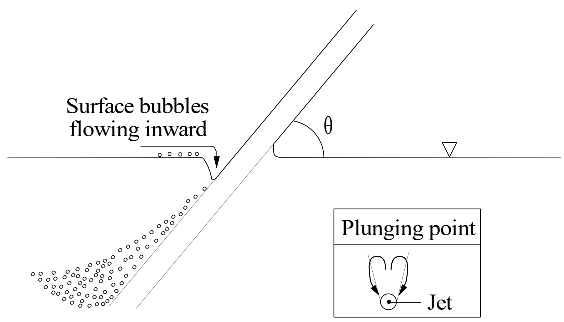

Figure 2. Angled water jet

3. EXPERIMENTAL

The experiments were carried out using an experimental apparatus at the Hydraulic Laboratory of the Faculty of Engineering, Firat University, Elazig, Turkey. A schematic representation of the experimental apparatus is shown in Figure 3. A series of laboratory experiments were conducted to measure the values of air entrainment rate (Q_a) in two-hole circular nozzles. The water in the experimental setup was circulated by a water pump through a flowmeter. The jet velocity at the nozzle inlet varied between 2.60 and 18.84 m/s. The nozzle diameter (D_0) was 14 mm, and the plunge angle of the water jet (θ) was 45˚. The length of the water jet (L_j) was chosen to be 10 cm, 20 cm, and 40 cm.

The experiments were conducted in a 1.8 m^3 glass wall water tank (0.75 m wide x 2.0 m long x 1.2 m high). An air hood with plan dimensions of 0.70 m x 0.75 m was used to determine the air entrainment rate values. A 16 mm diameter air vent was placed on top of the hood. A Testo 435 anemometer was used to measure the air velocity at the air vent on the hood. This measurement was made by placing the anemometer in the centre of the vent. Air velocity measurements were taken for 60 seconds or longer. The accuracy of the anemometer was ± (0.2 m/s + 1.5% of mv). The vertical orientation of the anemometer relative to the direction of flow in the vent was carefully considered to ensure accurate measurements. Once the air velocity was obtained, the air entrainment rate was calculated by multiplying the air velocity by the vent cross-sectional area. Water flow rates (Q_w) were measured using a calibrated electromagnetic flowmeter. A total of 252 experiments were conducted.

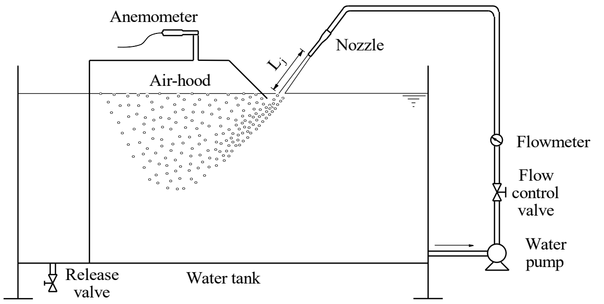

Figure 3. Experimental apparatus

Two air holes with diameters (D_1) of 2 mm, 4 mm, 6 mm, and 8 mm were drilled on the circular nozzle, as shown in Figure 4. A negative pressure (below atmospheric pressure - i.e., a vacuum) occurred at these air holes. This phenomenon also affected the jet expansion, jet shape, jet roughness, and air entrainment ratio. The length of the circular nozzle was chosen as L_n=2×D_0, 4×D_0, and 8×D_0.

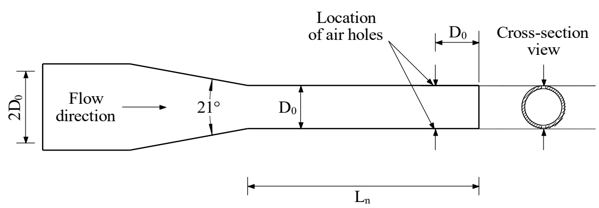

Figure 4. Two-hole circular nozzles

The Reynolds number was determined at the inlet of the nozzle because the cross-sectional area of the jet at the outlet of the nozzle changes as the air enters through the air holes (Equation 1).

$$\text{Reynolds number, Re} = \frac{We}{Ca} = \frac{\rho_w V_0 D_0}{\mu_w} \quad (1)$$

$$\text{Weber number, We} = \frac{\rho_w V_0^2 D_0}{\sigma} \quad (2)$$

$$\text{Capillary number, Ca} = \frac{\mu_w V_0}{\sigma} \quad (3)$$

where D_0 = jet diameter at nozzle inlet
V_0 = jet velocity at nozzle inlet
ρ_w = density
μ_w = dynamic viscosity
σ =interfacial tension.

4. RESULTS

The values of the air entrainment ratio of the two-hole circular nozzles were obtained experimentally as a function of the ratio of the nozzle diameter to the air hole diameter, the length of the water jet, the length of the circular nozzle, and the jet velocity at the nozzle inlet. The following sections are devoted to the presentation and discussion of the results.

A negative pressure drew air in through holes on circular nozzles. The resulting aeration of the jet affected its expansion, shape, roughness, and consequently the air entrainment ratio (Q_a/Q_w). The shape of the water jet was a narrow ellipse in two-hole circular nozzles. The air entrainment in the water jets issuing from the two-hole circular nozzles was sensitive to the Reynolds number (i.e., the water jet velocity at the nozzle inlet). Initially, a water jet with a relatively smooth surface was issued from the two-hole circular nozzles, and air entrainment occurred mainly at the surface of the water tank. As the water jet velocity at the nozzle inlet increased, the surface of the water jet issuing from the two-hole circular nozzles became roughened, entraining air as described by the rough jet mechanism. This resulted in more air flowing into the water tank.

The variation of the air entrainment ratio in the two-hole circular nozzles with Reynolds number is shown in Figure 5. The air entrainment ratio increased up to a Reynolds number of about 150000 and then decreased with a further increase in Reynolds number. The investigation showed that the maximum air entrainment ratio was achieved at a nozzle length that was four times the nozzle diameter. The minimum air entrainment ratio occurred at a nozzle length that was twice the nozzle diameter. For this nozzle, the air entrainment ratio showed minimal variation with Reynolds number.

The air hole diameter was found to have a significant effect on the air entrainment ratio. Higher air entrainment ratios were observed for air holes with diameters greater than 2 mm. The highest air entrainment ratio was 3.46. This value was obtained at a Reynolds number of approximately 150000, an air hole diameter of 4 mm, a nozzle length four times the nozzle diameter, and a water jet length of 400 mm.

The air entrainment ratio increased as the water jet length increased. The increase in air entrainment ratio with increasing water jet length can be attributed to increased jet expansion and jet roughness. For Reynolds numbers less than 60000, the effect of water jet length was not significant. Air entrainment mechanism 4, "droplet entrainment" as described by McKeogh and Ervine (1981), was not observed at any water jet length.

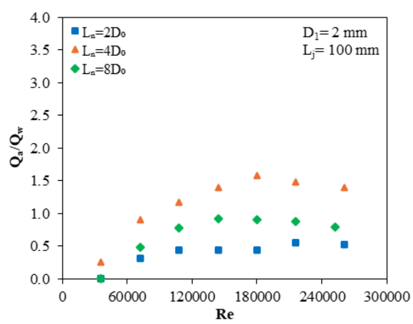

(a)

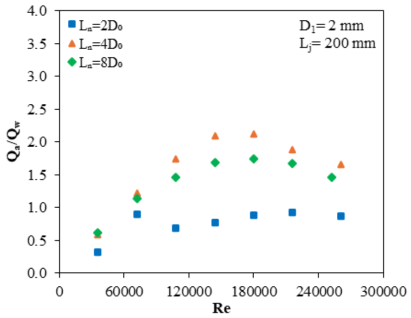
$L_a=2D_o$
$L_a=4D_o$
$L_a=8D_o$
D_j= 2 mm
L_j= 200 mm
Q_a/Q_w
Re
0.0 0.5 1.0 1.5 2.0 2.5 3.0 3.5 4.0
0 60000 120000 180000 240000 300000

(b)

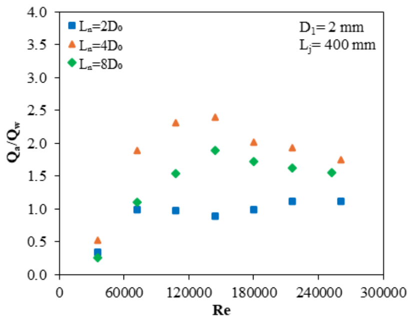
$L_a=2D_o$
$L_a=4D_o$
$L_a=8D_o$
D_j= 2 mm
L_j= 400 mm
Q_a/Q_w
Re
0.0 0.5 1.0 1.5 2.0 2.5 3.0 3.5 4.0
0 60000 120000 180000 240000 300000

(c)

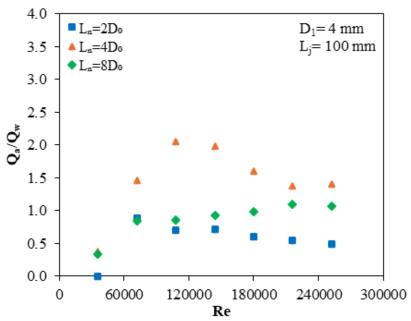
$L_a=2D_o$
$L_a=4D_o$
$L_a=8D_o$
D_j= 4 mm
L_j= 100 mm
Q_a/Q_w
Re
0.0 0.5 1.0 1.5 2.0 2.5 3.0 3.5 4.0
0 60000 120000 180000 240000 300000

(d)

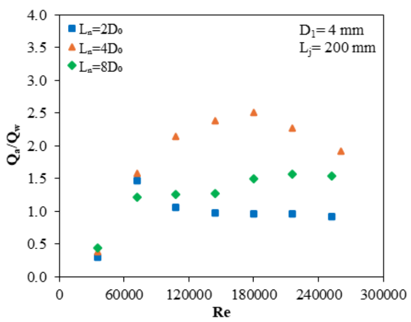
$L_a=2D_o$
$L_a=4D_o$
$L_a=8D_o$
D_j= 4 mm
L_j= 200 mm
Q_a/Q_w
Re
0.0 0.5 1.0 1.5 2.0 2.5 3.0 3.5 4.0
0 60000 120000 180000 240000 300000

(e)

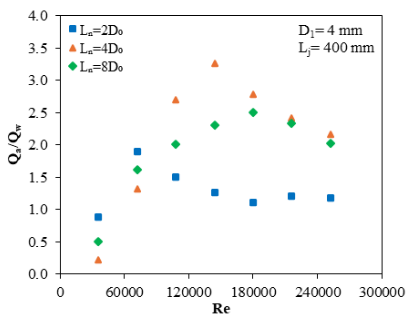
$L_a=2D_o$
$L_a=4D_o$
$L_a=8D_o$
D_j= 4 mm
L_j= 400 mm
Q_a/Q_w
Re
0.0 0.5 1.0 1.5 2.0 2.5 3.0 3.5 4.0
0 60000 120000 180000 240000 300000

(f)

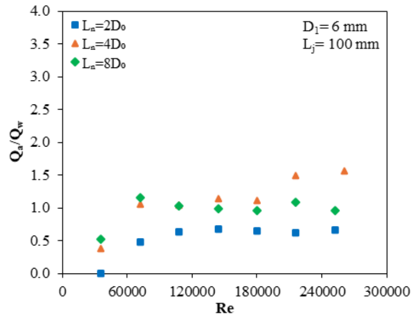
$L_a=2D_o$
$L_a=4D_o$
$L_a=8D_o$
D_j= 6 mm
L_j= 100 mm
Q_a/Q_w
Re
0.0 0.5 1.0 1.5 2.0 2.5 3.0 3.5 4.0
0 60000 120000 180000 240000 300000

(g)

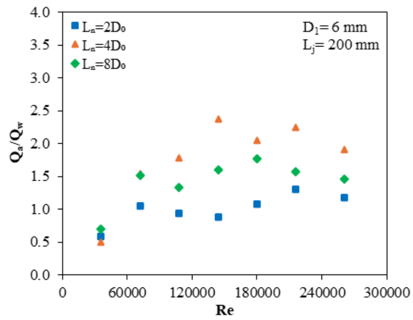
$L_a=2D_o$
$L_a=4D_o$
$L_a=8D_o$
D_j= 6 mm
L_j= 200 mm
Q_a/Q_w
Re
0.0 0.5 1.0 1.5 2.0 2.5 3.0 3.5 4.0
0 60000 120000 180000 240000 300000

(h)

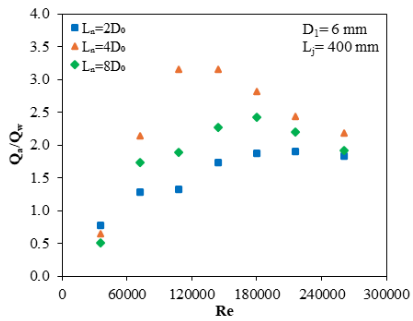
$L_a=2D_o$
$L_a=4D_o$
$L_a=8D_o$
D_j= 6 mm
L_j= 400 mm
Q_a/Q_w
Re
0.0 0.5 1.0 1.5 2.0 2.5 3.0 3.5 4.0
0 60000 120000 180000 240000 300000

(i)

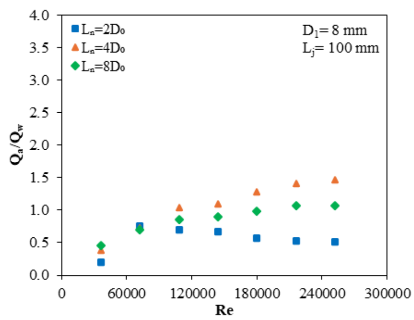
$L_a=2D_o$
$L_a=4D_o$
$L_a=8D_o$
D_j= 8 mm
L_j= 100 mm
Q_a/Q_w
Re
0.0 0.5 1.0 1.5 2.0 2.5 3.0 3.5 4.0
0 60000 120000 180000 240000 300000

(j)

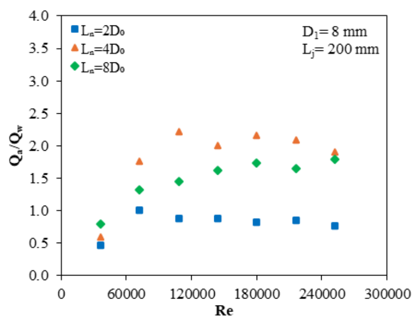
$L_a=2D_o$
$L_a=4D_o$
$L_a=8D_o$
D_j= 8 mm
L_j= 200 mm
Q_a/Q_w
Re
0.0 0.5 1.0 1.5 2.0 2.5 3.0 3.5 4.0
0 60000 120000 180000 240000 300000

(k)

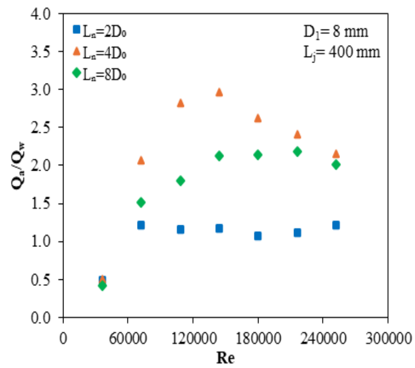

(l)

Figure 5. Q_a/Q_w versus Re for different values of L_n, L_j, and D_1

Regression analysis was performed using the nonlinear regression module. An empirical correlation was developed to predict the air entrainment ratio in two-hole circular nozzles. This prediction is based on the ratio of the nozzle diameter to the air hole diameter, the length of the water jet, the length of the circular nozzle, and the jet velocity at the nozzle inlet. The resulting correlation is shown in Equation (4) (Table 6). The 252 data points used in the study showed good agreement between the measured and predicted air entrainment ratios.

$$\frac{Q_a}{Q_w} = A + \left[B + C \times L_j{}^{D}\right]^{E} + \left[F + G \times L_n{}^{H}\right]^{I} + \left[J + K \times V_0{}^{L}\right]^{M} \qquad (4)$$

where: Q_a/Q_w = Air entrainment ratio
L_j = water jet length
L_n = circular nozzle length
V_0 = jet velocity at nozzle inlet
D_0 = nozzle diameter
D_1 = air hole diameter.

D_0/D_1	A	B	C	D	E	F	G	H	I	J	K	L	M	Correlation Coefficient
7.00	-1.386	-6.158	7.686	0.096	0.178	-9.049	12.938	0.100	0.076	-0.387	0.100	1.419	0.127	0.89
3.50	-1.769	-0.893	4.968	0.576	0.520	-1.310	4.971	0.373	0.076	-3.852	0.225	2.975	0.069	0.81
2.33	-1.944	0.386	1.134	0.248	2.923	-2.720	5.213	0.182	0.096	4.833	-6.435	-0.300	0.294	0.89
1.75	-1.012	-0.636	3.109	0.684	0.387	-0.400	6.166	0.765	0.120	-9.905	9.005	0.100	0.258	0.87

Table 6. Values of constants in Equation 4

5. CONCLUSIONS

A series of laboratory experiments were conducted to determine the air entrainment ratio values of the two-hole circular nozzles. The following results were obtained:

The air entrainment ratio increased up to a Reynolds number of about 150000 and then decreased with a further increase in Reynolds number.

The maximum air entrainment ratio was achieved with a nozzle length that was four times the diameter of the nozzle.

The air hole diameter was found to have a significant effect on the air entrainment ratio. Higher air entrainment ratios were observed for air holes with diameters greater than 2 mm.

The air entrainment ratio increased as the length of the water jet increased. At low Reynolds numbers, the effect of water jet length was not significant.

In addition, a design equation was developed to predict the air entrainment ratio in the two-hole circular nozzles as a function of the ratio of the nozzle diameter to the air hole diameter, the length of the water jet, the length of the circular nozzle, and the jet velocity at the nozzle inlet.

In the experiments conducted in this study, the jet velocities are generally consistent with the scale of the prototypes. However, it should be noted that the nozzle diameter may be smaller than in some prototype applications. Further experiments are needed to determine the effect of nozzle diameter on the air entrainment ratio.

Furthermore, future studies will contribute to a more comprehensive investigation of jet shape, penetration depth, and oxygen transfer efficiency in two-hole circular nozzles.

References

Alazmi, A., Al-Anzi, B.S. and Chiavola, A., 2023. Assessment of machine learning algorithms for predicting air entrainment rates in a confined plunging liquid jet reactor. *Sustainability*, 15(18), pp. 13802.

Bagatur, T. and Baylar, A., 1998. Aeration with water jets and practical applications. *DSI Technical Bulletin*, 92, pp. 17-29.

Bagatur, T., Baylar, A. and Sekerdag, N., 2002. The effect of nozzle type on air entrainment by plunging water jets. *Water Quality Research Journal of Canada*, 37(3), pp. 599-612.

Baylar, A. and Emiroglu, M.E., 2003. Air entrainment and oxygen transfer in a venturi. *Proceedings of the Institution of Civil Engineers - Water & Maritime Engineering*, 156(WM3), pp. 249-255.

Baylar, A. and Emiroglu, M.E., 2004. An experimental study of air entrainment and oxygen transfer at a water jet from a nozzle with air holes. *Water Environment Research*, 76(3), pp. 231-237.

Baylar, A., Aydin, M.C., Unsal, M. and Ozkan, F., 2008. CFD analysis to predict optimal air inlet hole diameter of venturi tube in terms of air injection. *e-Journal of New World Sciences Academy*, 3(2), pp. 211-224.

Baylar, A., Aydin, M.C., Unsal, M. and Ozkan, F., 2009. Numerical modeling of venturi flows for determining air injection rates using FLUENT V6.2. *Mathematical and Computational Applications*, 14(2), pp. 97-108.

Baylar, A., Emiroglu, M.E. and Ozturk, M., 2006. The development of aeration performance with different typed nozzles in a vertical plunging water jet system. *International Journal of Science and Technology*, 1(1), pp. 51-63.

Baylar, A., Ozkan, F. and Ozturk, M., 2005. Influence of venturi cone angles on jet aeration systems. *Proceedings of the Institution of Civil Engineers - Water Management*, 158(WM1), pp. 9-16.

Baylar, A., Ozkan, F. and Unsal, M., 2010a. Effect of air inlet hole diameter of venturi tube on air injection rate. *KSCE Journal of Civil Engineering*, 14(4), pp. 489-492.

Baylar, A., Ozkan, F. and Unsal, M., 2010b. Using venturi tubes in two-phase aeration processes. *International Sustainable Water and Wastewater Management Symposium*, pp. 378-386, Konya, Turkey.

Baylar, A., Ozkan, F. and Unsal, M., 2007a. On the use of venturi tubes in aeration. *CLEAN - Soil, Air, Water*, 35(2), pp. 183-185.

Baylar, A., Unsal, M. and Ozkan, F., 2007b. Determination of the optimal location of the air hole in venturi aerators. *CLEAN - Soil, Air, Water*, 35(3), pp. 246-249.

Bin, A. K., 1993. Gas entrainment by plunging liquid jets. *Chemical Engineering Science*, 48(21), pp. 3585-3630.

Emiroglu, M.E. and Baylar, A., 2003a. Role of nozzles with air holes in air entrainment by a water jet. *Water Quality Research Journal of Canada*, 38(4), pp. 785-795.

Emiroglu, M.E. and Baylar, A., 2003b. Study of the influence of air holes along length of convergent-divergent passage of a venturi device on aeration. *Journal of Hydraulic Research*, 41(5), pp. 513-520.

Evans, G. M., Jameson, G. J., and Rielly, C. D., 1996. Free jet expansion and gas entrainment characteristics of a plunging liquid jet. *Experimental Thermal and Fluid Science*, 12(2), pp. 142-149.

Fu, Z., Li, K., Pang, Y.J., Ma, L.Y., Wang, Z.Y. and Jiang, B., 2022. Study on water jet characteristics of square nozzle based on CFD and particle image velocimetry. *Symmetry-Basel*, 14(11), pp. 2392.

Kandukuri, K.R., Sucheendran, M.M. and Jampana, P., 2024. Detailed study of cavity features and air entrainment due to the initial impact of plunging jet flows. *Industrial & Engineering Chemistry Research*, 63(43), pp. 18586-18598.

Koga, M., 1982. Bubble entrainment in breaking wind waves. *Tellus*, 34(5), pp. 481-489.

Kusabiraki, D., Murota, M., Ohno, S., Yamagiwa, K. Yasuda, M., and Ohkawa, A., 1990a. Gas entrainment rate and flow pattern in a plunging liquid jet aeration system using inclined nozzles. *Journal of Chemical Engineering of Japan*, 23(6), pp. 704-710.

Kusabiraki, D., Niki, H, Yamagiwa, K., and Ohkawa, A., 1990b. Gas entrainment rate and flow pattern of vertical plunging liquid jets. *The Canadian Journal of Chemical Engineering*, 68(6), pp. 893-903.

Ma, Y., Zhang, L., Yang, Y. and Wei, P., 2020. Air entrainment by inclined circular plunging water jets with various impingement heights. *Water Supply*, 20(8), pp. 3478-3486.

McKeogh, E. J., and Ervine, D. A., 1981. Air entrainment rate and diffusion pattern of plunging liquid jets. *Chemical Engineering Science*, 36(7), pp. 1161-1172.

Miwa, S., Maribe, T., Tsutstumi, K. and Hibiki, T., 2018. Experimental investigation of air entrainment by vertical plunging liquid jet. *Chemical Engineering Science*, 181, pp. 251-263.

Miwa, S., Xiao, Y.G., Saito, Y. and Hibiki, T., 2019. Experimental study of air entrainment rates due to inclined liquid jets. *Chemical Engineering Technology*, 42(5), pp. 1059-1069.

Oguz, H. N., 1998. Role of surface disturbances in the entrainment of bubbles by a liquid jet. *Journal of Fluid Mechanics*, 372, pp. 189-212.

Ohl, C. D., Oguz, H. N., and Prosperetti, A., 2000. Mechanism of air entrainment by a disturbed liquid jet. *Physics of Fluids*, 12(7), pp. 1710-1714.

Ozkan, F., Baylar, A. and Tugal, M., 2006. The performance of two phase flow systems in pond aeration", *International Journal of Science and Technology*, 1(1), pp. 65-74.

Qu, X., Goharzadeh, A., Khezzar, L. and Molki., A. 2013. Experimental characterization of air-entrainment in a plunging jet. *Experimental Thermal and Fluid Science*, 44, pp. 51-61.

Salehi, F., Ajdehak, E. and Hardalupas, Y., 2022. Computational fluid dynamics modelling of air entrainment for a plunging jet. *Chemical Engineering Research and Design*, 179, pp. 319-330.

Sene, K. J., 1988. Air entrainment by plunging jets. *Chemical Engineering Science*, 43(10), pp. 2615-2623.

Tang, L., Wang, H. and Lin, P.Z., 2022. Numerical modeling of air entrainment by turbulent plunging jet and aerated flow in the plunging pool. *Environmental Fluid Mechanics*, 22(1), pp. 33-53.

van de Sande, E., and Smith, J. M., 1976. Jet break-up and air entrainment by low velocity turbulent water jets. *Chemical Engineering Science*, 31(3), pp. 219-224.

van de Sande, E., and Smith, J. M., 1973. Surface entrainment of air by high velocity water jets. *Chemical Engineering Science*, 28(5), pp. 1161-1168.

Yamagiwa, K., Ito, A., Tajima, K., Yoshida, M., and Ohkawa, A., 2000. Effect of nozzle contraction angle on air entrainment rate of a vertical plunging liquid jet. *Journal of Chemical Engineering of Japan*, 33(5), pp. 805-807.

Zhu, Y., Oguz, H. N., and Prosperetti, A., 2000. On the mechanism of air entrainment by liquid jets at a free surface. *Journal of Fluid Mechanics*, 404, pp. 151-177.